JOURNAL OF VIROLOGY, July 1997, p. 5040–5050 Vol. 71, No. 7
0022-538X/97/$04.00+0

Identification and Characterization of a Baculovirus Structural Protein, VP1054, Required for Nucleocapsid Formation

JULIE OLSZEWSKI[1] AND LOIS K. MILLER[1,2]*

Department of Genetics[1] and Department of Entomology,[2] University of Georgia, Athens, Georgia 30602

Received 4 December 1996/Accepted 24 March 1997

The defect in a temperature-sensitive mutant of *Autographa californica* nuclear polyhedrosis virus, *ts*N1054, was mapped and characterized. At the nonpermissive temperature of 33°C, this mutant fails to form plaques upon infection of Sf-21 cultured insect cells; infection is limited to a single cell, even though the infection proceeds through the very late phase. Marker rescue mapping and DNA sequencing identified the gene, ORF 54, which was altered by a single nucleotide substitution in *ts*N1054. Transcriptional analysis of the ORF 54 region identified multicistronic RNAs, from early to very late times of infection, that potentially encode the ORF 54 gene product. Polyclonal antiserum raised to a TrpE-VP1054 fusion protein recognized a 42-kDa late protein, VP1054, in infected-cell lysates. VP1054 was found to be a component of both budded virus and occlusion-derived virions. The level of VP1054 was dramatically reduced in *ts*N1054-infected Sf-21 cells propagated at 33°C, and electron microscopic analysis of these cells showed that nucleocapsids failed to form in the nuclei of these infected cells. Instead, novel round, electron-dense bodies were found associated with the virogenic stroma in *ts*N1054-infected cells. Therefore, VP1054 is a virus structural protein required for nucleocapsid assembly.

Baculoviruses are large, double-stranded, circular DNA viruses which are infectious to arthropods, primarily insects. *Autographa californica* nuclear polyhedrosis virus (Ac*M*NPV) is the most well characterized baculovirus, and its genome has been entirely sequenced (3). Ac*M*NPV replication produces two forms of progeny virus, an occluded form, which allows the virus to be transmitted from insect to insect through ingestion of contaminated food, and a budded form, which is responsible for dissemination of infection throughout the insect host (9, 15). The production of budded virus (BV) and occluded virus (OV) is the result of a complex cascade of gene regulation events (5, 28). Although the two viral forms are genetically identical, they have different morphologies, tissue tropisms, envelope sources, protein compositions, and temporal production (8, 32).

Baculovirus infection of cultured insect cells progresses in three phases, early, late, and very late. The transition from the early stage to late stage of infection is dependent upon viral DNA replication and occurs between 6 and 12 h after the initiation of infection. During the late phase of infection, newly replicated viral DNA is condensed and packaged within the nucleus, in association with the virogenic stroma, into capsid structures to form nucleocapsids. From about 12 to 20 h, these nucleocapsids leave the nucleus, travel through the cytoplasm, and bud through a modified plasma membrane to acquire a loosely fitting envelope important for BV infectivity (1, 26). Beginning at about 20 h, there is a transition from the late phase to very late phase of infection. Nucleocapsids remain within the nucleus, become bundled together, and are enveloped by a membrane elaborated within the nucleus (7, 13, 35). The resulting virions are embedded within a paracrystalline matrix, composed primarily of polyhedrin protein, to form OV.

Baculovirus structural proteins common to both or unique for one virion form have previously been identified (for reviews, see references 28 and 32). The nucleocapsid is the central component of both virion forms. With one possible exception (7), the same nucleocapsid proteins are found in both BV and occlusion-derived virions (ODV). The proteins identified as unique for BV or ODV are primarily associated with the envelope of each form (6, 7, 14, 32, 36, 40). We report here the identification of a new baculovirus structural protein, VP1054, which is the first to be demonstrated as essential for nucleocapsid assembly.

A temperature-sensitive (*ts*) mutant virus of Ac*M*NPV, *ts*N1054, was originally isolated by chemical mutagenesis with *N*-methyl-*N*′-nitro-*N*-nitrosoguanidine and a subsequent screen for *ts* phenotypes (18). *ts*N1054 exhibits a single-cell infection phenotype of cultured Sf-21 insect cells at the nonpermissive temperature of 33°C. Individual cells proceed through infection to the very late phase, as evidenced by the presence of occlusion bodies that are visible in the nuclei of these cells by light microscopy. However, plaques are not formed so there is an impediment to the spread of virus to neighboring cells (18).

Marker rescue mapping and DNA sequencing identified the *ts* mutation in ORF 54 of Ac*M*NPV. Characterization of the product of ORF 54, VP1054, identified a 42-kDa protein contained within BV and ODV. Western analysis of the *ts* version of VP1054 demonstrated that the protein failed to accumulate to wild-type (wt) levels at 33°C. Electron microscopic analysis of *ts*N1054-infected cells at 33°C revealed the total absence of nucleocapsids in these cells, but unusual structures associated with the virogenic stroma were observed.

MATERIALS AND METHODS

Cells and virus. The L1 (wt) strain of Ac*M*NPV was propagated in the IPLB Sf-21 (Sf-21) cell line (38) at 27°C. The *ts*N1054 mutant virus was propagated in Sf-21 cells adapted for growth at 23°C (permissive temperature) (28). Sf-21 cells adapted for growth at 33°C (nonpermissive for *ts*N1054) were also used in some studies. All cell lines were grown in TC-100 medium (GIBCO/BRL, Gaithersburg, Md.) with 10% fetal bovine serum and 0.26% tryptose broth (28).

Plasmid constructs. (i) The Ac*M*NPV genomic library lambda clone, PstHI, was subcloned into Bluescript II KS+ (Stratagene, La Jolla, Calif.) to generate plasmid pPstHI. The construction of pPstHI and its subclones, pPstHI XhoI, pPstHI Stu 3.3, and pPstHI Sal 0.65, has been described elsewhere (22). Plasmid

* Corresponding author. Mailing address: Department of Entomology, 413 Biological Sciences Bld., The University of Georgia, Athens, GA 30602. Phone: (706) 542-2294. Fax: (706) 542-2279. E-mail: miller@bscr.uga.edu.

pBSRIN consists of Ac*M*NPV DNA from the *Eco*RI site at 32.7 map units (m.u.) to the *Eco*RI site at 34.5 m.u. in Bluescript II KS+ at its *Eco*RI site. Plasmid pPstHI Eco 1.4 (33.6 to 34.8 m.u.) (22) was digested with *Not*I and *Eco*RI, and the 985-bp fragment was cloned into Bluescript II KS+ to create pPstHI NE 1.0 (33.8 to 34.5 m.u.). Plasmid pPstHI Eco 1.4 was also digested with *Cla*I, which cuts once at 34.0 m.u., and *Eco*RI, which cuts in the Bluescript II KS+ multiple cloning site and at 34.5 m.u. This generated two Ac*M*NPV fragments of 665 and 765 bp. Bluescript II KS+ was digested with *Eco*RI and *Cla*I, and both the 765- and 667-bp fragments were inserted separately to create pPstHI ECl 0.76 (33.5 to 34.0 m.u.) and pPstHI ClE 0.66 (34.0 to 34.5 m.u.), respectively.

(ii). *ts*N1054 viral DNA was digested with *Eco*RI, and the sequence corresponding to the *Eco*RI-N fragment (32.9 to 34.8 m.u.) was cloned into the *Eco*RI site in Bluescript KS+. This plasmid, p*ts*54 RI-N, was digested with *Cla*I and *Eco*RI, and the resulting 665-bp fragment (34.3 to 34.8 m.u.) was cloned into Bluescript II KS+ to create p*ts*54 C1E 0.66. This clone was constructed to be the *ts* equivalent of the wt clone for this region, pPstHI C1E 0.66.

(iii). To construct the TrpE-VP1054 fusion protein construct, plasmid pPstHI NE 1.0 was cut with *Hin*dIII (which cuts in the Bluescript II KS+ multiple cloning site) and partially digested with *Sal*I. A 730-bp fragment comprised of Ac*M*NPV sequence from the *Sal*I site at 34.0 m.u. to the *Eco*RI site at 34.5 m.u. was gel purified and ligated into vector pATH-3 (16) which had also been digested with *Sal*I and *Hin*dIII. pATH-3 contains the N-terminal coding sequence of the *Escherichia coli trpE* gene, which, fused to VP1054 coding sequence corresponding to amino acids 116 to 353, generates a fusion protein product of ~58 kDa (32 kDa from TrpE and ~26 kDa from VP1054) in *E. coli* XL-1 Blue cells (Stratagene). This clone, which encodes 237 of the 365 total amino acids of the VP1054 protein, represents approximately two-thirds of ORF 54.

Marker rescue experiments. The *ts*N1054 mutation was first mapped by using a library of overlapping Ac*M*NPV genomic clones (29) and then mapped further with the plasmid subclones described above. Marker rescue experiments were performed with Sf-21 cells adapted for growth at 33°C, which were plated at a density of 2×10^6 cells per 60-mm-diameter tissue culture dish. Lambda or plasmid clones (5.0 μg/plate) and *ts*N1054 viral DNA (0.5 μg/plate) were cotransfected by the Lipofectin method according to the manufacturer's (GIBCO/BRL) protocol. Cells were incubated with a mixture of DNA, Lipofectin, and TC-100 medium without serum at 33°C for 4 h and then washed with TC-100 medium without serum. Cells were overlaid with agarose as previously described (28) and then maintained at 33°C. Plates were scored 4 to 5 days later for the presence of plaques after a subsequent agarose overlay containing neutral red.

DNA sequencing. The smallest plasmid DNA subclone which tested positive for marker rescue, pPstHI C1E 0.66, and the equivalent clone from *ts*N1054, p*ts*54 C1E 0.66, were sequenced. One strand of each plasmid was sequenced by the dideoxynucleotide chain termination method (34), and the complementing strands were sequenced by fluorescent DNA sequencing at the Molecular Genetics Instrumentation Facility (University of Georgia, Athens).

Production of polyclonal serum. The TrpE-VP1054 fusion protein plasmid construct was grown in XL-1 Blue cells and induced to produce the fusion protein as previously described (16). The fusion protein, found in the insoluble fraction of cell lysates, was visualized by light staining with Coomassie blue 250 (Sigma Chemical Co., St. Louis, Mo.) in water (12) after separation by sodium dodecyl sulfate-polyacrylamide gel electrophoresis (SDS-PAGE) (17). The portion of the polyacrylamide gel containing the fusion protein was excised and ground with a Dounce homogenizer. The homogenate was injected into rabbits at the Animal Resources Facility (University of Georgia) to produce polyclonal antiserum to VP1054.

Western analysis. Sf-21 cells, at a density of 2×10^6 cells per 60-mm-diameter dish, were mock infected or infected with wt or *ts*N1054 virus at a multiplicity of infection (MOI) of 10 PFU per cell as previously described (28). At each time point, cells were washed off the plate with TC-100 medium without serum, pelleted at $1,000 \times g$ for 5 min, washed once with 1 ml of insect phosphate-buffered saline (pH 6.2) (1 mM $Na_2HPO_4 \cdot 7H_2O$, 10.5 mM KH_2PO_4, 140 mM NaCl, 40 mM KCl), and repelleted. Cells were resuspended in 0.5 ml of 2× SDS buffer (0.125 M Tris [pH 6.8], 4.0% SDS, 20.0% glycerol, 10.0% 2-mercaptoethanol, 0.002% bromophenol blue) supplemented with a protease inhibitor cocktail (Pharmingen, San Diego, Calif.) and stored until use at −70°C. Samples were boiled for 5 min, and 2 μl (~8,000 cells) was then subjected to SDS-PAGE through either a 10 or 12% polyacrylamide running gel with a 5.2% stacking gel (17). Proteins were electrophoretically transferred to a polyvinylidene difluoride membrane and visualized with a chemiluminescence detection kit (ECL kit; Amersham, Arlington Heights, Ill.). VP1054 antiserum or preimmune serum was diluted 1:5,000 in Tris-buffered saline (pH 7.6) with 0.1% Tween 20 (Sigma Chemical Co.) according to the manufacturer's protocol. To detect major capsid protein VP39, rabbit polyclonal antiserum (37) or preimmune serum was used at a 1:8,000 dilution. In all cases, mouse anti-rabbit antibody conjugated with horseradish peroxidase (Promega) was utilized as a secondary antibody at a 1:25,000 dilution. MultiMark colored protein standards (Novex Experimental Technology, San Diego, Calif.) were used to approximate protein sizes. The BV used in Western analysis was harvested from the medium of wt virus-infected cells and purified by isopycnic centrifugation on a 25 to 60% sucrose step gradient as previously described (28). ODV were purified from wt virus-infected Sf-21 larvae by isopycnic centrifugation on a 40 to 65% sucrose step gradient as previously described (28). BV and ODV were resuspended in 2× SDS buffer and analyzed as described above.

Metabolic labeling of proteins. Sf-21 cells, adapted for growth at 33°C and at a density of 10^6 cells per 35-mm-diameter dish, were mock infected or infected with wt or *ts*N1054 virus at an MOI of 10. At each time point, cells were incubated in medium lacking cysteine and methionine for 1 h and then the medium was replaced with medium supplemented with 25 μCi of Tran^{35}S label (ICN, Irvine, Calif.), which has a mixture of [^{35}S]methionine and [^{35}S]cysteine. The radioactive medium was removed after 1 h, and cells were lysed in 50 μl of 2× SDS buffer with protease inhibitors and boiled for 5 min. SDS-PAGE was performed with 6 μl of each lysate, and the gel was processed for fluorography (24).

RNA isolation. Total cellular RNA was isolated from mock-infected and wt virus-infected Sf-21 cells grown at 27°C. Cells were infected at an MOI of 10 by adsorbing virus for 1 h at room temperature. Fresh TC-100 medium with serum was added to each plate, which was then incubated at 27°C for the indicated time (in hours) from the addition of fresh medium. A separate plate was adsorbed with virus for 1 h, treated with aphidicolin (5 μg/ml) in fresh medium, and harvested 12 h later. RNA was prepared with TRI reagent (Molecular Research Center, Cincinnati, Ohio), and all samples were treated with RQ-1 DNase (Promega). Poly(A)$^+$ mRNA selection was performed with Oligotex purification minipreps (Qiagen, Chatsworth, Calif.) according to the manufacturer's specifications.

Northern analysis. Poly(A)$^+$ RNA (0.75 μg per lane) was denatured by glyoxalation (25) and electrophoresed through a 1.2% agarose gel as previously described (28). Ethidium bromide-stained RNA and DNA marker ladders (GIBCO/BRL) were used to approximate transcript sizes. RNA was electrophoretically transferred to a Zeta-Probe nylon blotting membrane (BIO-RAD, Melville, N.Y.) and UV cross-linked. Plasmid pPstHI C1E 0.66 was digested with *Cla*I and *Eco*RI, and a 665-bp fragment was gel isolated and radiolabeled by nick translation (24) for the detection of ORF 54 transcripts. Northern blot hybridization was done at 42°C overnight as previously described (28).

S1 nuclease analysis. To map the 3′ ends of ORF 54 transcripts, a double-stranded plasmid, pPstHI Stu 3.3, was digested with *Xho*I and the 3′ ends were labeled in the presence of Klenow fragment and [α-^{32}P]dCTP. This fragment was cut again with *Sal*I, and a 1.4-kb fragment, corresponding to nucleotides 46,231 to 47,665 (34.5 to 35.6 m.u.) in the Ac*M*NPV genome, was gel isolated. This probe, along with 50 μg of total RNA, was denatured at 70°C for 20 min in the presence of 80% formamide–40 mM PIPES [piperazine-*N*,*N*′-bis(2-ethanesulfonic acid] (pH 6.4)–400 mM NaCl–1 mM EDTA (pH 8.0) and allowed to anneal at 47°C overnight. After hybridization, S1 nuclease (300 U), S1 buffer (0.28 M NaCl, 0.1 M sodium acetate [pH 4.5], 4.5 mM $ZnSO_4$), and 6 μg of salmon sperm DNA were added, and the mixture was incubated at 30°C for 1 h. S1 nuclease-resistant fragments were heat denatured and analyzed by separation in polyacrylamide-urea gels. To map the 5′ ends of ORF 54 transcripts, plasmid pBSRIN was digested with *Pvu*II, a 2.2-kb fragment was gel isolated, and the 5′ ends were phosphorylated with T4 polynucleotide kinase in the presence of [γ-^{32}P]ATP. This fragment was further digested with *Eco*RI, generating a 2.2-kb probe containing sequence corresponding to nucleotides 43,800 to 45,999 (32.7 to 34.3 m.u.).

Primer extensions. Two oligonucleotides were designed to map the 5′ ends of ORF 54 transcripts. A 29-nucleotide oligomer, PREXT54-1 (5′-CTAACTTGA TCGGTTTCTTGGTCGAACAC-3′), that spans nucleotides 45,224 to 45,252 of Ac*M*NPV and a 21-nucleotide oligomer, PREXT54-4 (5′-CGAAGCATCACG TTGCACTCC-3′), that corresponds to nucleotides 44,981 to 45,001 were phosphorylated at their 5′ ends with T4 polynucleotide kinase and [γ-^{32}P]ATP. Primer extension reaction mixtures included 100 fmol of radiolabeled primer and 50 μg of total RNA from mock-infected or wt virus-infected cells harvested at 12 h. Primer extension reactions were performed by using the avian myeloblastosis virus reverse transcriptase primer extension system (Promega) according to the manufacturer's protocol. Extension products were ethanol precipitated, resuspended in 8 μl of loading dye (Promega), and denatured by boiling, and 4 μl of each sample was analyzed on an 8% polyacrylamide–urea gel. The extension products were visualized by autoradiography. The oligomers described above were also used as primers to sequence the corresponding DNA of plasmid pBSRIN by the dideoxynucleotide chain termination sequencing method (34) to allow precise determination of the start sites.

Electron microscopy. Sf-21 cells were mock infected or infected at an MOI of 10 with wt or *ts*N1054 virus and propagated at 33°C. At 16 h, cells were collected, washed with TC-100 medium lacking serum, and pelleted at $1,000 \times g$ for 5 min. Cell pellets were resuspended and fixed in a solution of 5% glutaraldehyde with 0.1 M tetrabutylammonium fluoride in 0.025 M HEPES buffer (pH 7.2). After a 1-h incubation at room temperature, cells were washed twice with HEPES buffer and pelleted in a microcentrifuge for 30 s. Pellets were resuspended in a solution of 1% osmium tetroxide in 0.025 M phosphate buffer (pH 7.4) with 0.1 M potassium fluoride (KF). Cells were incubated for 1 h at 4°C, pelleted, and rinsed twice in phosphate buffer. Cells were resuspended for 10 min in each of the following in a dehydration series: 50% acetone (with 0.1 M KF), 70% acetone (with 0.1 M KF), 80% acetone (with 0.05 M KF), 95% acetone, 100% acetone (twice), and 100% propylene oxide. Cells were embedded in Epon, sectioned, and negatively stained with uranyl acetate and lead citrate. Samples were viewed

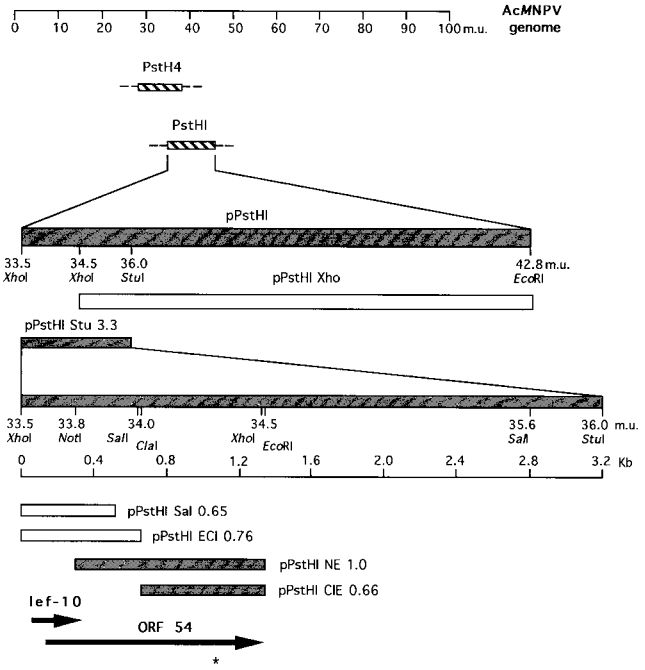

FIG. 1. Marker rescue mapping of the mutation in *ts*N1054. Sf-21 insect cells were cotransfected with *ts*N1054 viral DNA and lambda genomic DNA clones derived from wt virus, two of which rescued *ts*N1054 and are represented by hatched boxes, with approximate endpoints indicated by dashes. Plasmid subclones were also tested. Shaded boxes indicate fragments from plasmid clones that rescued the *ts* phenotype; open boxes represent those that did not rescue. Rescue by homologous recombination was scored by the ability of fragments to produce viruses which could form plaques. Arrows indicate the positional direction of *lef 10* and ORF 54. An asterisk marks the location of the *ts* mutation, as determined by DNA sequencing (Fig. 2). One map unit is ~1.34 kb.

with a JEOL 100CX II transmission electron microscope at an accelerating voltage of 80 kV.

RESULTS

Mapping of the *ts*N1054 mutation. The location of the mutation in *ts*N1054 was initially delimited by marker rescue. Insect (Sf-21) cells were cotransfected with *ts*N1054 viral DNA and clones of wt Ac*M*NPV (29) that overlap and collectively span the entire Ac*M*NPV genome. Transfection of *ts*N1054 DNA alone did not generate viruses which could form plaques at 33°C. However, homologous recombination between the defective portion of *ts*N1054 viral DNA and the corresponding wt Ac*M*NPV sequence upon cotransfection reconstructed a wt virus which formed plaques at 33°C. Rescue of the single-cell infection phenotype was scored by the presence of plaques 4 to 5 days after transfection. Two overlapping lambda clones, PstH4 and PstHI, were able to rescue *ts*N1054 (Fig. 1); all other Ac*M*NPV genomic clones (not depicted) were not able to rescue *ts*N1054. A plasmid clone of the PstHI region, containing Ac*M*NPV sequence from 33.5 to 42.8 m.u., also rescued *ts*N1054. A plasmid subclone of this region, pPstHI Xho (34.5 to 42.8 m.u.), did not rescue, but plasmid pPstHI Stu 3.3 (33.5 to 36.0 m.u.), which corresponds to the leftmost region of pPstHI, rescued the *ts* phenotype. Further subclones from this region, such as pPstHI Sal 0.65 and pPstHI ECl 0.76, did not rescue the defect. Plasmid pPstHI C1E 0.66, which contains 667 bp of Ac*M*NPV sequence from nucleotides 45,614 to 46,281, was the smallest region to provide reproducible positive rescue. The average number of plaques (from three independent experiments) resulting from cotransfecting pPstHI C1E 0.66 and *ts*N1054 viral DNA was 25 ± 5 per plate, while *ts*N1054 viral DNA transfected alone resulted in no plaques being formed. The major open reading frame in this region of Ac*M*NPV is ORF 54, as defined by Ayres et al. in their description of open reading frames for Ac*M*NPV (3), which predicts a 42-kDa polypeptide.

Sequencing of 34.0 to 34.5 m.u. of wt Ac*M*NPV and *ts*N1054. The plasmid with wt Ac*M*NPV sequence, pPstHI C1E 0.66, and the corresponding *ts*N1054 plasmid, p*ts*54 C1E 0.66, were each sequenced from both strands. One nucleotide difference was found between these two sequences; it was a change of C to T at position 1427 (Fig. 2). This corresponds to nucleotide 46,077 in the Ac*M*NPV sequence (3) and lies within the ORF 54 coding sequence. There are no other open reading frames of >50 codons in this region of the Ac*M*NPV genome from alternate reading frames or encoded by the other strand. This substitution alters the first position of the codon from CCG to TCG. Instead of a proline at residue 286, the product of ORF 54 is predicted to contain serine. Within this sequenced region, one nucleotide difference between the C6 strain of Ac*M*NPV and the parental strain of *ts*N1054, the L1 strain, was found at what corresponds to nucleotide 1448 (Fig. 2). The nucleotide reported for this position in the C6 strain (nucleotide 46,098) is a T in the first position of the codon, TTT, which encodes phenylalanine at amino acid 293 of the predicted ORF 54 product. In both L1 and *ts*N1054, this nucleotide is a G and the GTT codon is predicted to encode valine. This is a conservative amino acid substitution, and since it was found to be the same in L1 and *ts*N1054 on both strands, it can be ruled out as the cause of the *ts* phenotype.

Transcription mapping of the ORF 54 region of Ac*M*NPV. We were interested in mapping ORF 54 transcript(s) and determining the temporal regulation of ORF 54 transcription. This was of interest because the nucleotide sequence directly upstream of the first ATG of ORF 54 has neither the early motif (CAGT) nor late motif (TAAG) typically associated with baculoviral transcription start sites. The nearest motifs are three clustered TAAG sites, the closest of which is 523 bp upstream of the first ATG of ORF 54 (Fig. 2). In addition, the *lef 10* coding sequence overlaps with the last codon of ORF 53 and the first 47 codons of ORF 54 (Fig. 2 and 3), and the possibility of a bi- or tricistronic transcript adds to the potential complexity of transcription and translation from this region.

Northern analysis was performed with poly(A)$^+$ selected RNA from mock- or wt virus-infected Sf-21 cells at 6, 12, 24, and 48 h. The radiolabeled probe used was the *Cla*I-to-*Eco*RI fragment from pPstHI C1E 0.66 (Fig. 3). A total of six RNAs were detected throughout the time course (Fig. 4A). A transcript of ~1.9 kb was first detected at 6 h, increased to its maximum level at 12 h, decreased by 24 h, and was barely detectable by 48 h. Two transcripts, one of ~2.3 kb and another of ~3.0 kb, were detected at 12 h and persisted through 48 h. Two additional transcripts, of approximately 5.0 and 6.0 kb, were present at low levels at 24 h but were more abundant at 48 h, suggesting very late transcriptional regulation. An additional transcript of ~1.5 kb was detected at 12 h. For a control, cells were adsorbed with wt virus for 1 h before treatment with aphidicolin, an inhibitor of DNA replication, and these cells were collected 12 h later (Fig. 4A, lane 12A). Since late viral gene expression requires DNA replication, only early viral transcripts are present in these cells, even though they are harvested at the late time of 12 h. Only the 1.9-kb transcript was detected, confirming that the 1.9-kb RNA is an early transcript and that all of the other transcripts are strictly late or very late transcripts that are dependent on viral DNA replication.

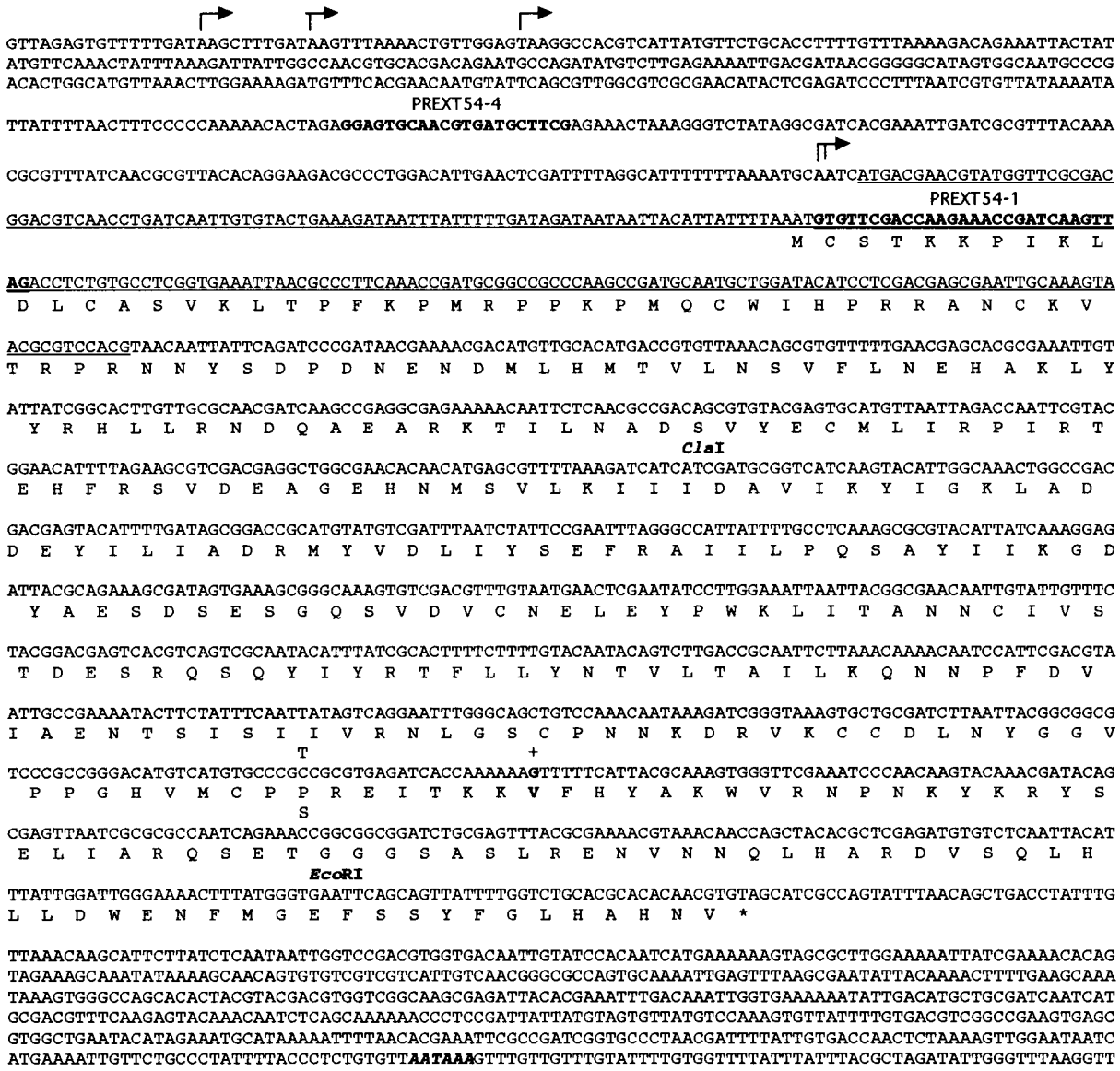

FIG. 2. Nucleotide sequences of wt Ac*M*NPV and *ts*N1054 DNAs from 44,651 to 46,950 (33.3 to 35.0 m.u.). The *Cla*I-to-*Eco*RI rescuing DNA fragment from the L1 strain of Ac*M*NPV and the corresponding sequence from *ts*N1054 were sequenced, and the one nucleotide difference, a C-to-T change, is indicated above the L1 sequence. The resulting change of a proline to a serine is indicated in the one-letter amino acid code below the nucleotide sequence. One difference was found between the C6 and L1 strains of Ac*M*NPV and is indicated in bold type with a plus sign above it at position 1448. Nucleotide one corresponds to nucleotide 44,651 in Ac*M*NPV. Bold numbers represent amino acids from ORF 54. Sequences upstream and downstream of the *Cla*I-to-*Eco*RI region (sites indicated above sequence) are from the C6 strain of Ac*M*NPV (3) and were not sequenced by us (except in the immediate vicinity of transcription start sites which were identical in both sequences). Sites where oligonucleotide primers anneal are labeled and in bold, and transcription start sites are indicated by arrows. A consensus polyadenylation site (AATAAA) near the 3′ ends of ORF 54 transcripts is shown in bold italics.

S1 nuclease mapping was used to map the 3′ ends of ORF 54 transcripts. The 3′ probe was a 1.4-kb fragment from pPstHI Stu 3.3 radiolabeled at the *Xho*I site at nucleotide 46,231 within the C terminus of ORF 54 and extending to the *Sal*I site at nucleotide 47,665 (Fig. 3). The probe was incubated with total RNA from mock- or wt virus-infected cells, treated with S1 nuclease, and subjected to electrophoresis. One major protected fragment, which migrated with a 650-nucleotide size standard, was detected at 6, 12, 24, and 48 h (Fig. 4B). This positions the 3′ end approximately 565 nucleotides downstream of the ORF 54 termination codon and correlates with a consensus polyadenylation site at position 2240 (Fig. 2). This polyadenylation site is also the predicted stop codon for ORF 56. The 6- and 24-h lanes also had a protected fragment corresponding to the full-length probe (Fig. 4B). Because a double-stranded DNA probe was used for these studies, the complementary DNA strand can compete with RNA for annealing to the labeled DNA strand, even at elevated temperatures. This seemed to be the case for the 3′ end probe because the appearance of a full-length protected band was variable from experiment to experiment as well as from lane to lane (data not shown), although the possibility of a 3′ end further downstream of the *Sal*I site cannot be ruled out.

S1 mapping of the 5′ ends was performed with an *Eco*RI-to-*Pvu*II fragment from plasmid pBSRIN radiolabeled at the 5′ end of the *Pvu*II site (at nucleotide 45,999) within the C ter-

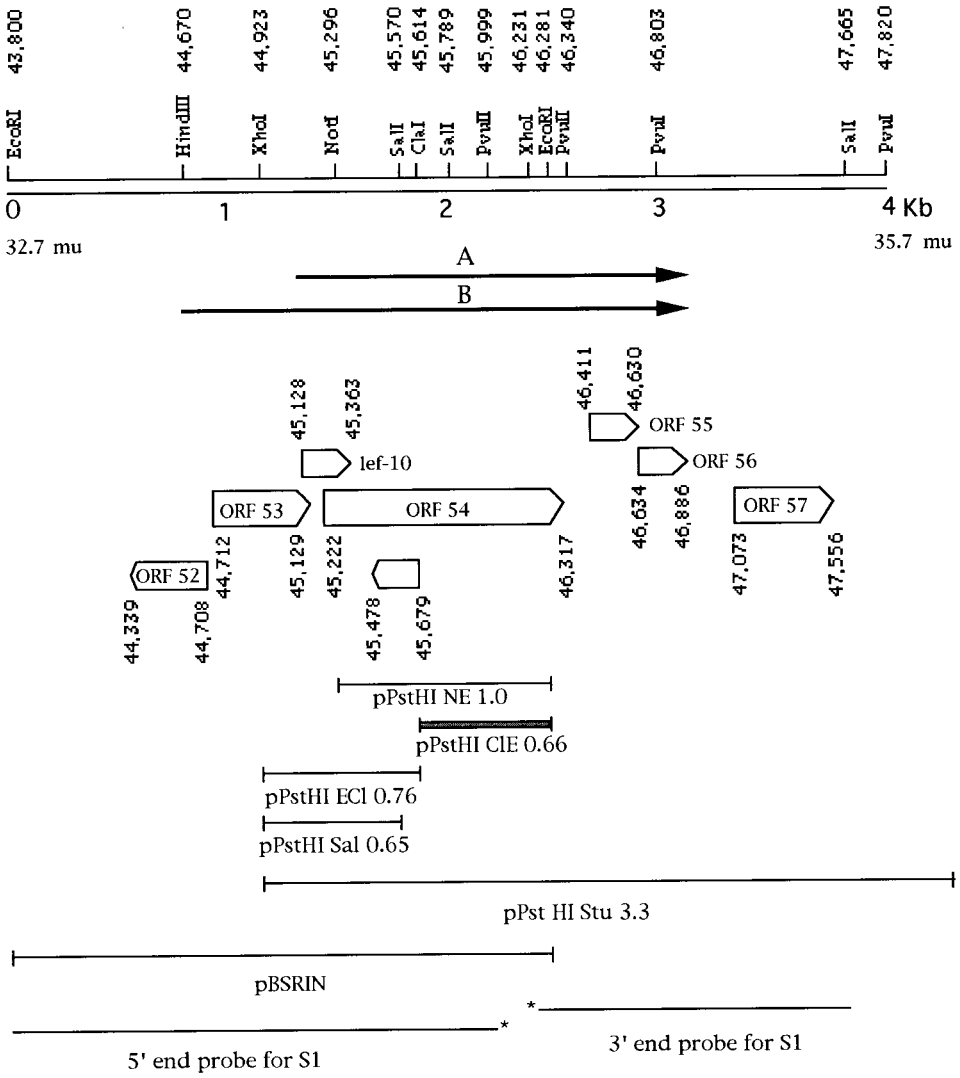

FIG. 3. Schematic diagrams of potential open reading frames of Ac*M*NPV from 32.7 to 35.7 m.u. For convenience, the Ac*M*NPV genome is represented as a linear molecule by double lines with relevant restriction sites indicated above and numbered according to their positions relative to the entire Ac*M*NPV genomic sequence (3). Open reading frames are depicted as open arrows, with pointed ends indicating directionality relative to the Ac*M*NPV genome. The probes used for S1 nuclease analysis are shown, with an asterisk indicating the radiolabeled end (5′ or 3′). Remaining single lines represent the regions contained within plasmids that were used for marker rescue analysis or to create probes for RNA analysis. The Ac*M*NPV sequence from plasmid pPstHI C1E 0.66 used for Northern analysis is indicated by a shaded box.

minus of ORF 54 and extending 2,196 nucleotides to the *Eco*RI site at 43,800 (Fig. 3). Total RNA from wt virus-infected cells (12 and 24 h), but not mock-infected RNA, resulted in two major protected fragments of about 850 and 1,400 nucleotides (data not shown). The 850-nucleotide fragment corresponds to a site about 80 nucleotides upstream of the ORF 54 ATG, possibly near the ATG of *lef 10*. The 1,400-nucleotide fragment corresponds to a 5′ end about 600 nucleotides upstream of the ORF 54 ATG and within 100 nucleotides of the ATG of ORF 53. A protected fragment corresponding to the protected full-length probe was consistently observed with RNA from infected cells but not from mock-infected cells (data not shown) and probably corresponds to RNA(s) initiated further upstream.

Primer extension analysis of 5′ ends of ORF 54 transcripts. To more accurately define the 5′ ends of ORF 54 transcripts, primer extensions were performed with mock-infected and 12-h RNA from wt virus-infected Sf-21 cells. An oligonucleotide primer (PREXT54-1) that is complementary to nucleotides 574 to 602 (Fig. 2) and corresponds to nucleotides 3 to 31 of ORF 54 was used for mapping the proximal 5′ end seen with S1 mapping (Fig. 5A). Two major 5′ ends (Fig. 5A), occurring 97 and 98 nucleotides away from the primer at two consecutive A nucleotides, were detected with RNAs from infected cells, not from mock-infected cells. These 5′ ends are 99 and 100 nucleotides upstream of the ATG of ORF 54 and 3 and 4 nucleotides upstream of the first ATG of *lef 10* (Fig. 2). This corresponds well to the smaller protected fragment seen by S1 mapping of the 5′ end and, along with the 3′ end mapping data, predicts a transcript of ~1.8 kb. This transcript could potentially encode not only *lef 10* and ORF 54 but ORF 55 and ORF 56 as well and probably corresponds to the prominent ~1.9-kb transcript [1.8 kb plus a poly(A) tail] detected by Northern analysis at 12 h (Fig. 4A).

Additional larger extension products were observed with 12-h RNA (Fig. 5A), indicating that some ORF 54 transcripts

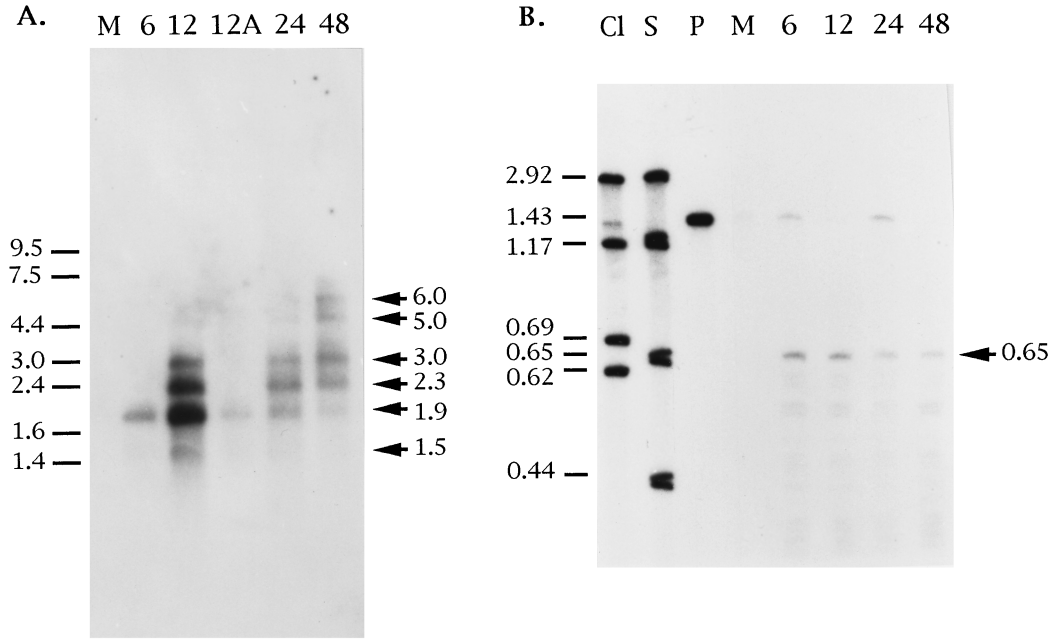

FIG. 4. Northern blot analysis and S1 nuclease mapping of the 3′ ends of RNAs transcribed from the ORF 54 region of Ac*M*NPV. (A) Poly(A)$^+$ selected RNAs from mock- (M) and wt virus-infected Sf-21 cells were harvested at the indicated times (in hours) and were subjected to Northern analysis with a nick-translated probe from pPstHI C1E 0.66 (see Materials and Methods). Lane 12A, control in which aphidicolin was added to the infection to prevent the synthesis of late transcripts which are dependent on DNA replication. The sizes (in kilobases) of RNA and DNA standards, which were visualized by ethidium bromide staining, are indicated on the left. The approximate sizes of RNAs are indicated by arrows on the right. (B) Total RNAs from mock- and wt virus-infected Sf-21 cells were subjected to S1 nuclease treatment in the presence of an *Xho*I-to-*Sal*I 3′ end probe. Protected fragments were electrophoresed through a 4% polyacrylamide–urea gel, and a major protected fragment of 650 nucleotides, detected by autoradiography, is indicated by an arrow. P, untreated full-length probe. Size standards were prepared by digestion of labeled pBSRIN with *Xho*I and *Cla*I (C1) or with *Xho*I and *Sal*I (S) and are shown on the left.

initiate even further upstream of *lef 10*. The extension products observed might be minor transcriptional start sites but are more likely due to premature chain termination during primer extension because no S1-protected fragments corresponding to these sites were found and splicing of baculovirus RNAs is rare. Because the PREXT54-1 primer anneals at the very N-terminal portion of the ORF 54 coding sequence, an additional primer, PREXT54-3, which is complementary to nucleotides 669 to 688 (Fig. 2), was used for primer extension reactions and the same two 5′ ends were detected with no additional 5′ ends observed (data not shown).

A third oligonucleotide primer was used to map the more distal 5′ end(s) represented by the larger of the two protected fragments seen with S1 analysis. This oligonucleotide primer, PREXT54-4, contains the sequence complementary to nucleotides 331 to 351 (Fig. 2) and corresponds to nucleotides 269 through 289 of ORF 53. Primer extension with this probe (Fig. 5B) showed three 5′ ends from within the three TAAG sequences upstream of ORF 53 (Fig. 2). Based upon the relative amounts of extension products observed with this primer, the middle TAAG site is the predominant start site, with smaller amounts of RNA from the other two TAAG sites. These three 5′ ends correspond well to the larger protected fragment seen with 5′ S1 end mapping. Only one protected fragment, instead of three, was seen with S1 analysis within this size range because of the close proximity of the start sites and the size of the probe. Transcripts from these TAAG sites which terminate at the site detected by the 3′ probe would yield a transcript of ~2.2 kb and could potentially encode ORF 53, *lef 10*, ORF 54, ORF 55, and ORF 56. A transcript of ~2.3 kb was detected by Northern analysis at 12 h and fits this prediction (Fig. 4A). The ~3.0-kb transcript detected by Northern analysis at 12 h is predicted to initiate further upstream than our 5′ S1 probe was designed to detect and was not investigated further.

Characterization of the ORF 54 protein, VP1054. A TrpE-VP1054 fusion construct containing the N-terminal coding sequence of the bacterial *trpE* gene fused to amino acids 116 to 353 of ORF 54 was designed. This construct was induced to express the fusion protein in *E. coli*, and antibodies were raised in rabbits inoculated with the gel-purified fusion protein. Western blot analysis of wt virus-infected cell lysates revealed an ~42-kDa polypeptide which was cross-reactive with this polyclonal antiserum (Fig. 6A). This protein was absent from mock-infected cell lysates and cells harvested at 6 h but was detected at 12 to 48 h. This agrees with the molecular mass, 42,094 Da, predicted for the polypeptide encoded by ORF 54. As a negative control, preimmune rabbit serum was also tested; it did not detect this 42-kDa protein (Fig. 6A).

In order to determine whether the 42-kDa protein is present in the virions of wt virus, BV and ODV were purified by centrifugation through sucrose gradients and subjected to SDS-PAGE and Western analysis (Fig. 6B). The 42-kDa protein was present in both BV and ODV and migrated at the same size as the protein detected from infected-cell lysates at 24 h (Fig. 6B). Polyclonal immune serum to major capsid protein VP39 (37) was used as a control for loading equivalent numbers of nucleocapsids from BV and ODV (Fig. 6C). Preimmune serum controls for both the 42-kDa protein encoded by ORF 54 and VP39 are shown in Fig. 6B and C. We refer to this 42-kDa protein as VP1054, indicating that it is a virus structural protein originally identified through analysis of the mutant *ts*N1054 and also providing a reminder of its correspondence to ORF 54.

We next examined by Western blot analysis VP1054 expres-

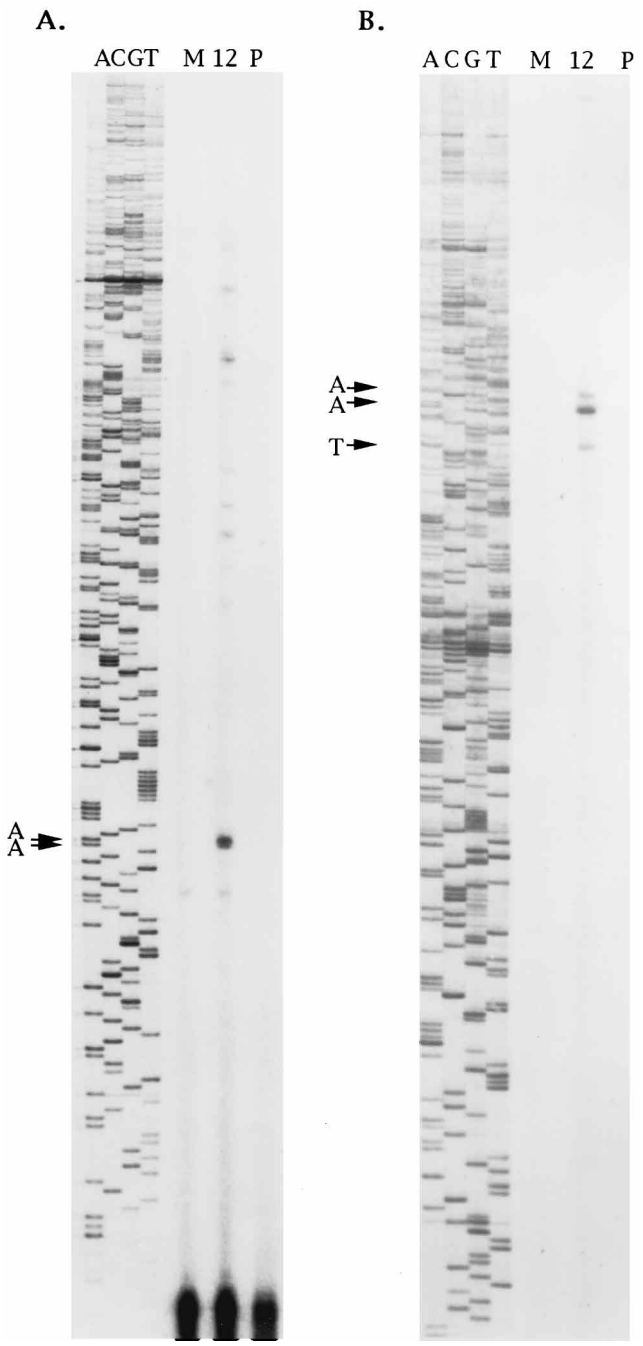

FIG. 5. Primer extension analysis of ORF 54 transcripts. Total RNAs from mock-infected (M) and wt virus-infected Sf-21 cells at 12 h (12) were incubated with oligonucleotide primers PREXT54-1 (A) and PREXT54-4 (B) to map precisely the proximal and distal 5′ ends, respectively, of ORF 54 transcripts with avian myeloblastosis virus reverse transcriptase. Extension products were separated by electrophoresis through an 8% polyacrylamide–urea gel. The same primers were used to sequence pBSRIN plasmid DNA to generate ladders (lanes A, C, G, and T) for precise determination of 5′ ends. Arrows denote 5′ ends. P, primers incubated without RNA.

sion in wt virus- and *ts*N1054-infected cells at 33°C at various times after infection (Fig. 7A). While VP1054 was present in both wt virus- and *ts*N1054-infected cells at 12 h, the amount of protein from *ts*N1054-infected cells was reduced compared to that of wt virus-infected cells. By 24 and 48 h, VP1054 could not be detected from *ts*N1054-infected cell lysates. The most likely explanation for this result is that the mutant version of VP1054 is unstable at high temperatures and is quickly turned over; therefore, it cannot accumulate to normal levels. This same blot was stripped and reprobed with the VP39 immune serum (Fig. 7B) to show that both the loading of cell lysates and the extent of infection of these cells were equivalent for wt virus and *ts*N1054 infections. The VP39 amounts in wt virus- and *ts*N1054-infected cell lysates were similar. To determine whether this severe reduction in VP1054 protein was, in fact, temperature dependent, wt virus and *ts*N1054 infections at 23°C were analyzed in the same manner. The amount and kinetics of VP1054 protein expression in lysates of wt virus- and *ts*N1054-infected cells at the permissive temperature were similar (Fig. 7C).

Protein profiles from metabolic labeling of wt virus- and *ts*N1054-infected cells at 33°C. Although VP39 production appeared to be normal in mutant infections at 33°C (Fig. 7B), we wanted to determine whether the failure of VP1054 to accumulate at 33°C in *ts*N1054-infected cells was specific for this protein. Mock-, wt virus-, and *ts*N1054-infected cells were pulse-labeled with radioactive cysteine and methionine at various times postinfection at 33°C in order to radioactively label the proteins being synthesized at these times. Cells were harvested after labeling, and lysates were subjected to SDS-PAGE and fluorography to produce a protein profile for each infection (Fig. 8). Both wt virus- and *ts*N1054-infected cells showed profiles characteristic of Ac*M*NPV infection of Sf-21 cells. Temporally regulated viral proteins were detected from 12 through 48 h, with a gradual shutoff of host protein synthesis. By 48 h, the predominant protein synthesized was polyhedrin, which migrated to ~32 kDa (Fig. 8). Although the overall regulation of protein expression was retained in *ts*N1054-infected cells at 33°C, beginning at 24 h, differences in the intensities of two protein bands between wt virus- and *ts* virus-infected cells were observed. The positions of the two proteins that were more abundant in wt virus-infected cells than in *ts*N1054-infected cells at 24 h are indicated in Fig. 8. These differences appear to be greater than can be accounted for as a variation in sample loading. The identities of these proteins were not investigated further, but the larger one migrated with the molecular mass (42 kDa) expected for VP1054. The smaller band may represent a breakdown product of VP1054 since low-molecular-weight bands can be detected by Western analysis if cell lysates are not handled carefully.

Electron microscopic analysis of *ts*N1054-infected Sf-21 cells at 33°C. VP1054 is a component of both BV and ODV and is thus likely to function as a structural protein of the nucleocapsid. If VP1054 is a structural protein, then the lack of VP1054 in *ts*N1054-infected cells at 33°C could affect the formation or infectivity of virus particles. Since *ts*N1054 has a single-cell infection phenotype at 33°C, there could be a total defect in BV production or noninfectious particles could be produced. To address this question, Sf-21 cells were mock infected or infected with wt virus or *ts*N1054 at 33°C, harvested at 16 h (during the exponential phase of BV production for Ac*M*NPV), and processed for electron microscopic analysis (Fig. 9). wt virus- and *ts*N1054-infected cells (Fig. 9B through D) could be easily distinguished from uninfected cells (Fig. 9A) by the presence of the virogenic stroma, which is an electron-dense, baculovirus-induced structure seen within the nucleus. The virogenic stroma is thought to be the active site for viral DNA replication, condensation, and packaging into capsids (10, 13, 43). Nucleocapsids are usually observed at the electron-dense edges of the stroma and occasionally seem to be in the process of acquiring a condensed core of DNA (10).

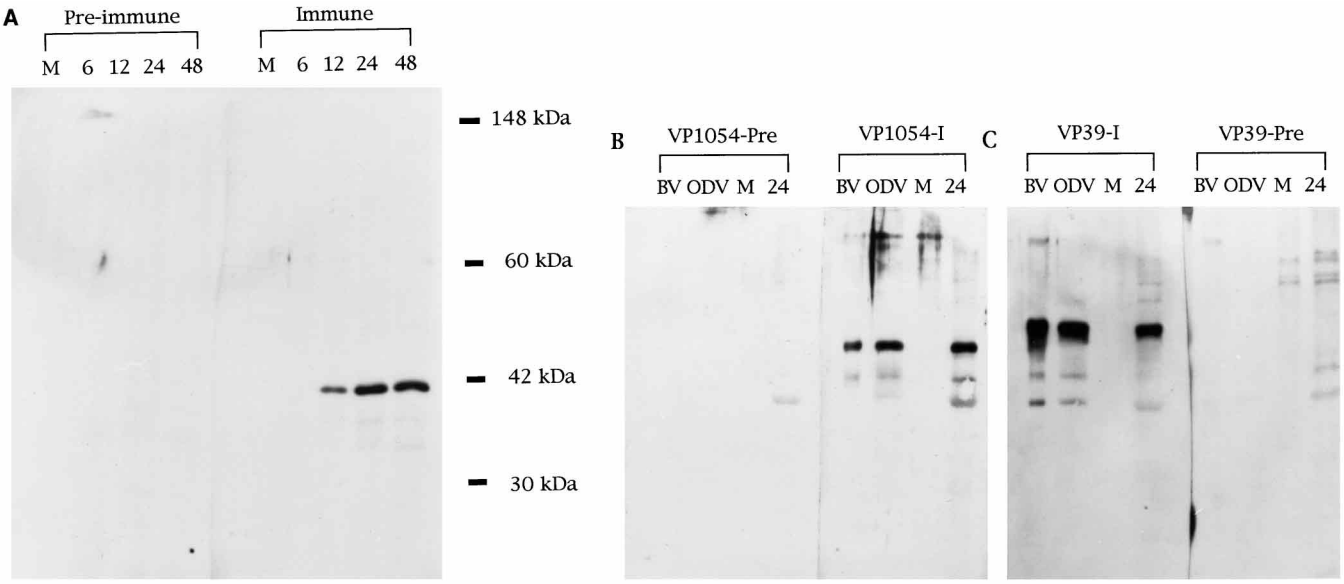

FIG. 6. Western analysis detects an Ac*M*NPV protein, VP1054, in infected-cell lysates and virus particles. (A) Mock (M) and wt virus-infected Sf-21 cell lysates from a time course (in hours) were subjected to SDS-PAGE. Proteins were transferred to a polyvinylidene difluoride membrane and probed with rabbit polyclonal sera. The left half of the membrane was probed with rabbit preimmune serum, and the right half was probed with polyclonal immune serum raised against the TrpE-VP1054 fusion protein. Protein size standards are indicated. (B) Sucrose gradient-purified BV and ODV along with mock- and wt virus-infected-cell lysates at 24 h were subjected to SDS-PAGE and Western analysis. The left gel was probed with rabbit preimmune serum (VP1054-Pre), and the right gel was probed with immune serum raised against the TrpE-VP1054 fusion protein (VP1054-I). (C) The lysates were the same as those for panel B, but the left gel was probed with immune serum to capsid protein VP39 (VP39-I) and the right gel was probed with rabbit preimmune serum (VP39-Pre).

wt virus-infected cells at 33°C showed nucleocapsids associating with the virogenic stroma, as well as progressing out of the nucleus, passing through the cytoplasm (Fig. 9B and C), and budding through the plasma membrane (data not shown). However, all *ts*N1054-infected cells propagated at 33°C (Fig. 9D) completely lacked nucleocapsids. Novel spherical structures with electron-dense surfaces (Fig. 9D) were associated with the virogenic stroma in *ts*N1054-infected Sf-21 cells (Fig. 9D) but not wt virus-infected Sf-21 cells at 33°C (Fig. 9C). Although the virogenic stroma appears to be more extensive in the *ts*N1054-infected cell nucleus than in the wt virus-infected cell nucleus, this is just a function of the plane of section for this particular wt virus-infected cell nucleus and does not reflect a general trend.

DISCUSSION

Marker rescue experiments and DNA sequencing revealed a single nucleotide difference between the smallest wt rescuing fragment and the equivalent region from *ts*N1054. This C-to-T transition was consistent with the chemical mutagen, *N*-methyl-*N*′-nitro-*N*-nitrosoguanidine, which facilitates G/C-to-A/T substitutions during DNA replication. This nucleotide change predicted an alteration at the amino acid level in VP1054, changing the proline at position 286 to a serine. Replacing proline with serine is expected to alter the folded structure of the polypeptide and could explain the apparent instability of mutant VP1054 at the nonpermissive temperature.

Northern analysis of the ORF 54 region from wt virus-infected cells detected six RNAs. A transcript of ~1.9 kb was detected early, before viral DNA replication, and the remaining transcripts were detected at late or very late times. S1 nuclease analysis of the 3′ ends of these transcripts detected only one 3′ end in this region, approximately 565 nucleotides downstream of the ORF 54 termination codon. S1 nuclease analysis of the 5′ ends detected two 5′ ends, approximately 80 and 600 nucleotides upstream of the ATG of ORF 54, as well as additional RNA(s) initiating further upstream. Primer extension results confirmed the presence of a 5′ end corresponding to the smaller protected fragment seen with S1 analysis of 5′ ends. This 5′ end was not located within consensus early or late baculovirus transcription initiation sites but would correspond to the 1.9-kb RNA species seen at both early and late times by Northern analysis.

The larger protected S1 fragment corresponded to initiation of transcription from three clustered TAAG sites located just upstream of ORF 53, as determined by primer extension analysis. These three transcripts would correspond to the 2.3-kb RNA species first seen at late times by Northern analysis and are probably multicistronic, including ORF 53, *lef 10*, ORF 54, ORF 55, and ORF 56. The larger RNA species in this region (e.g., 3.0, 5.0, and 6.0 kb) were detected by Northern analysis but were not characterized further. A transcript unique to ORF 54 was not identified, nor is it the 5′-proximal ORF of any of the transcripts in this region. We do not know the mechanism by which VP1054 is translated from one or more of these transcripts. Perhaps internal initiation of translation allows for expression of downstream genes of these multicistronic RNAs. The number of overlapping transcripts suggests a complex system for gene regulation in this region, and translational studies of this region could prove to be interesting.

Polyclonal antiserum to a TrpE-VP1054 fusion protein identified a 42-kDa polypeptide from wt virus-infected cell lysates. VP1054 was first detected by Western analysis at 12 h, accumulated to its maximum level by 24 h, and continued to be present at this level through at least 48 h. This type of temporal expression is characteristic of a baculovirus late protein. Since VP1054 was found in both BV and ODV, it is likely a component of the nucleocapsid since this is the one structure common to these virion forms. Furthermore, we have demon-

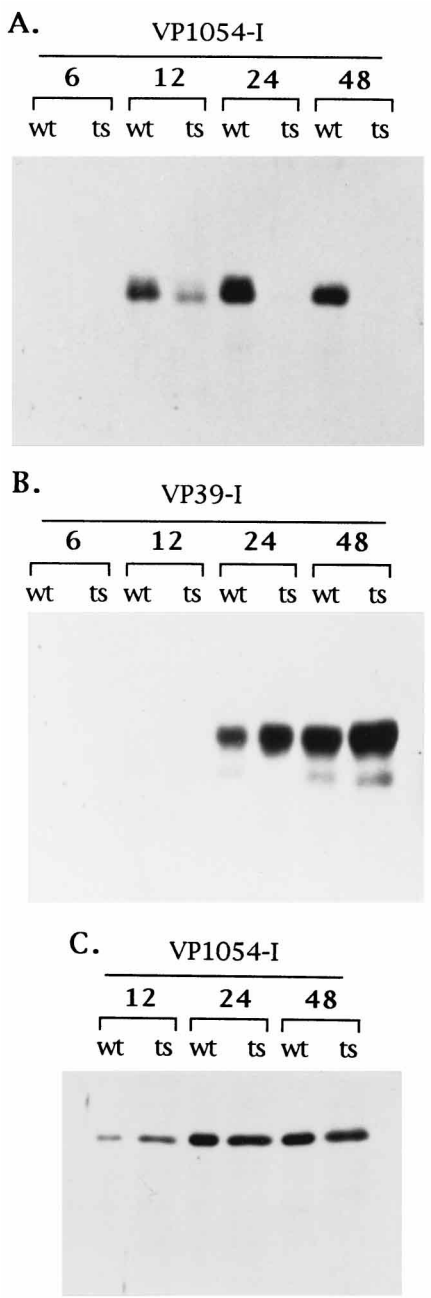

FIG. 7. VP1054 is stably expressed in *ts*N1054-infected cells at 23°C but not at 33°C, as determined by Western blot analysis. (A) Cell lysates from wt virus (wt)- and *ts*N1054 (ts)-infected cells propagated at 33°C were harvested at the indicated times (in hours), subjected to Western blot analysis, and probed with VP1054 immune serum (VP1054-I). (B) The blot in panel A was stripped and reprobed with capsid VP39 immune serum (VP39-I). (C) wt- and *ts*N1054-infected cells propagated at 23°C and lysates were subjected to Western analysis with VP1054 immune serum.

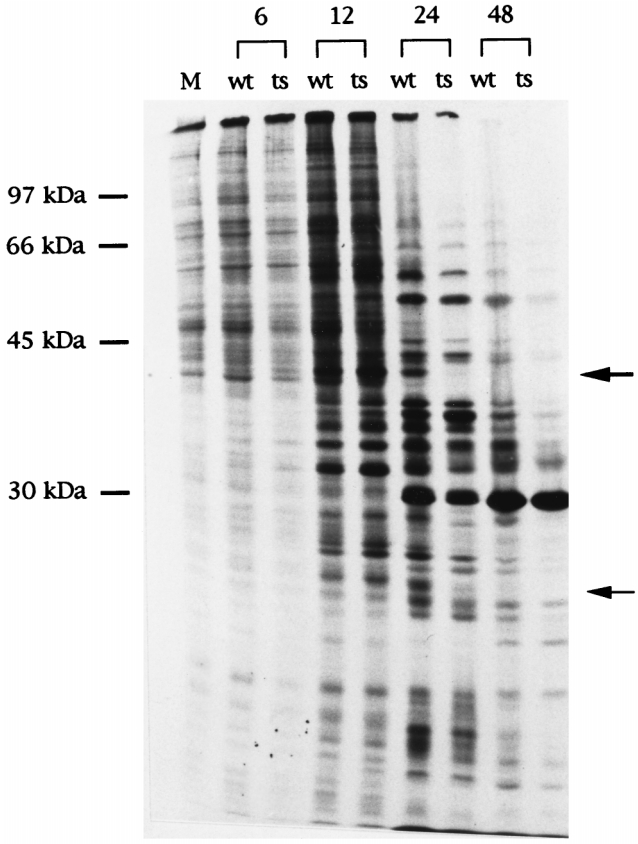

FIG. 8. Metabolic labeling of mock-, wt virus-, and *ts*N1054-infected Sf-21 cell proteins. Mock-, wt virus-, and *ts*N1054-infected cells at 33°C were pulse-labeled at the indicated times for 1 h in the presence of radioactively labeled cysteine and methionine to label newly synthesized proteins and then harvested. Cell lysates were electrophoresed through an SDS–12% polyacrylamide gel and processed for fluorography. Size standards are indicated on the left, and arrows indicate differences in protein synthesis between wt virus- and *ts*N1054-infected cells at 24 h.

strated that nucleocapsids fail to assemble in *ts*N1054-infected cells at the restrictive temperature. Nucleocapsid assembly precedes the acquisition of envelopes by both BV and ODV, providing additional evidence that VP1054 must be a component of the nucleocapsid.

Database searches at both nucleotide and amino acid levels were performed with VP1054 sequences by using the BLAST program (2). The only homologous sequence identified was from a closely related baculovirus, *Bombyx mori* nuclear polyhedrosis virus. The Ac*M*NPV and *Bombyx mori* nuclear polyhedrosis virus (GenBank accession no. L33180) sequences have 96% identity at the nucleotide level within ORF 54.

Metabolic labeling of newly synthesized proteins in wt virus- and *ts*N1054-infected cells at 33°C appeared to yield identical protein profiles through 12 h. Beginning at 24 h, however, differences in the levels of two proteins were clearly observed between wt virus and the *ts* mutant, with the *ts* infection producing less labeled protein than did wt infection. One of these proteins was probably VP1054; the identity of the other is not known, but it may be a breakdown product of VP1054. The instability of VP1054 at 33°C was observed by Western blot analysis of steady-state levels of this protein and is consistent with this hypothesis.

Identification and characterization of mutants defective in virus structural proteins afford us the opportunity to gain an understanding of the events associated with virus assembly. The novel structures associated with the virogenic stroma of *ts*N1054-infected cells at the nonpermissive temperature may be a direct result of the failure of nucleocapsids to be properly assembled. If this is the case, these structures could represent virus structural protein accumulation sites. Immunogold labeling experiments using antibodies that recognize Ac*M*NPV

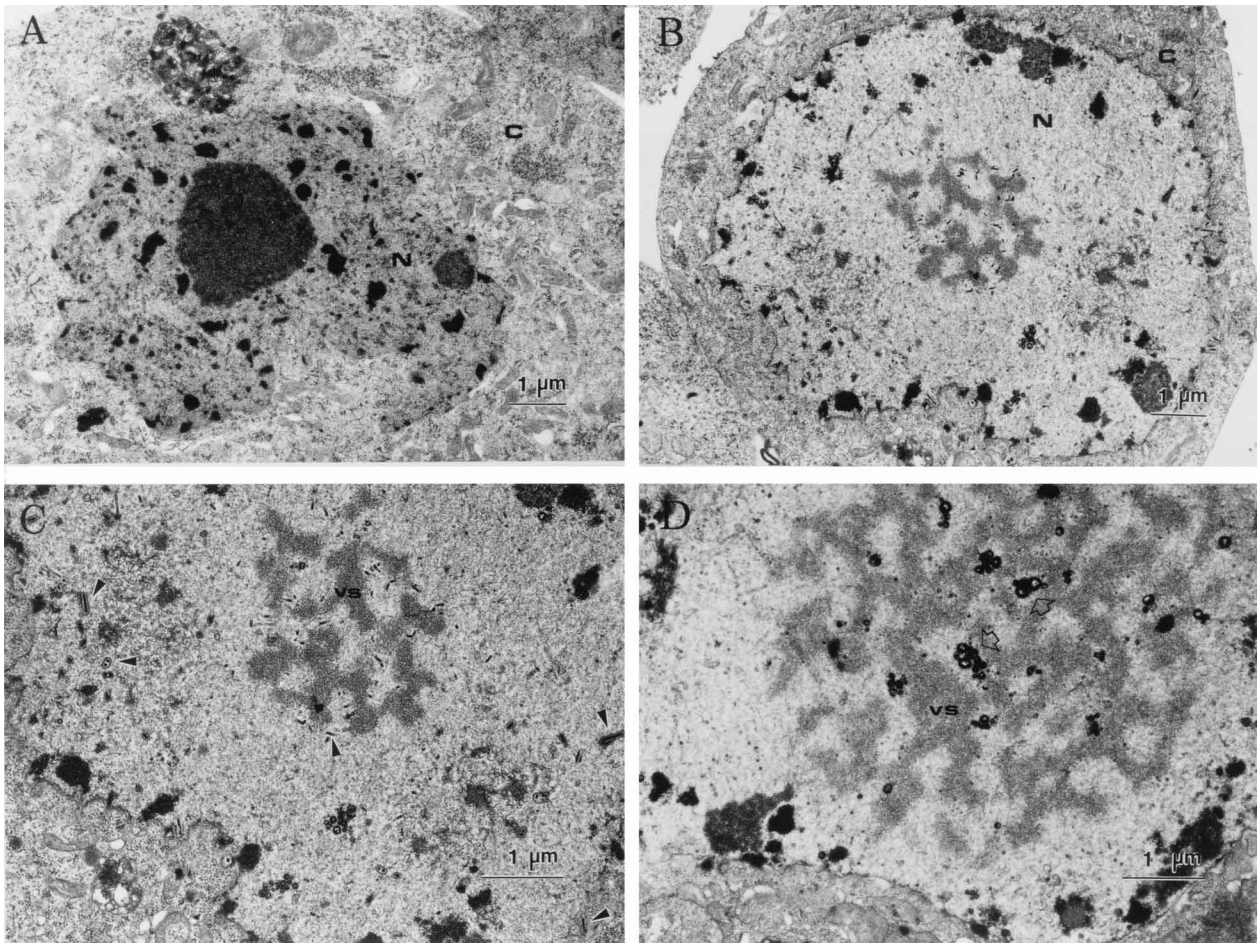

FIG. 9. Electron micrographs of mock-, wt virus-, and *ts*N1054-infected Sf-21 cells at 33°C. Mock (A)- and wt virus (B)-infected Sf-21 cells, with the cytoplasmic (C) and nuclear (N) regions designated. (C) A higher magnification of the cell in panel B, in which the virogenic stroma (vs) and representative nucleocapsids (arrowheads) are indicated. (D) A *ts*N1054-infected Sf-21 cell, showing the virogenic stroma (vs) but lacking nucleocapsids. Novel structures (open arrows) are found associated with the *ts*N1054-infected cell virogenic stroma. Scale bar, 1 μm. Panels C and D are magnified 1.5-fold relative to panels A and B.

structural proteins could potentially delineate the component(s) of these unusual structures.

Baculovirus proteins found to be associated with both BV and ODV include the major capsid protein (VP39) (4, 30, 37), basic protamine-like protein p6.9 (23, 33, 41), capsid-associated p87 protein (21, 27), p78/83 phosphoprotein/ORF 1629 (31, 39), capsid-associated p24 protein (11, 42), and protein tyrosine phosphatase/ORF 21 (19, 20). VP1054, therefore, joins the growing list of proteins that are associated with both BV and ODV, although it is the first baculovirus protein shown directly to be required for nucleocapsid assembly.

ACKNOWLEDGMENTS

We thank A. Lorena Passarelli for constructing the pBSRIN and Albert Lu for constructing members of the pPstHI plasmid series. We also thank Cathy Kelloes at the Electron Microscopy Laboratory, University of Georgia, for assistance with the electron microscopy work and Nickie Cauthen for critical review of the manuscript.

This work was supported in part by Public Health Service grant AI23719 from the National Institute of Allergy and Infectious Diseases to L.K.M. and in part by National Institute of Health predoctoral traineeship GM07103 to J.O.

REFERENCES

1. **Adams, J. R., R. H. Goodwin, and T. A. Wilcox.** 1977. Electron microscopic investigations on invasion and replication of insect baculoviruses *in vivo* and *in vitro*. Biol. Cell. **28:**261–268.
2. **Altschul, S., W. Gish, W. Miller, E. Myers, and D. Lipman.** 1990. Basic local alignment search tool. J. Mol. Biol. **215:**403–410.
3. **Ayres, M. D., S. C. Howard, J. Kuzio, M. Lopez-Ferber, and R. D. Possee.** 1994. The complete DNA sequence of *Autographa californica* nuclear polyhedrosis virus. Virology **202:**586–605.
4. **Blissard, G. W., R. L. Q. Russell, G. F. Rohrmann, and G. S. Beaudreau.** 1989. Nucleotide sequence transcriptional mapping and temporal expression of the gene encoding p39 a major structural protein of the multicapsid nuclear polyhedrosis virus of Orgyia pseudotsugata. Virology **168:**354–362.
5. **Blissard, G. W., and G. F. Rohrmann.** 1990. Baculovirus diversity and molecular biology. Annu. Rev. Entomol. **35:**127–155.
6. **Braunagel, S., D. Elton, H. Ma, and M. Summers.** 1996. Identification and analysis of an *Autographa californica* nuclear polyhedrosis virus structural protein of the occlusion-derived virus envelope: ODV-E56. Virology **217:** 97–110.
7. **Braunagel, S., H. He, P. Ramamurthy, and M. Summers.** 1996. Transcription, translation, and cellular localization of three *Autographa californica* nuclear polyhedrosis virus structural proteins: ODV-E18, ODV-E35, and ODV-EC27. Virology **222:**100–114.
8. **Braunagel, S. C., and M. D. Summers.** 1994. *Autographa californica* nuclear polyhedrosis virus, PDV, and ECV viral envelopes and nucleocapsids: structural proteins, antigens, lipid and fatty acid profiles. Virology **202:**315–328.
9. **Engelhard, E. K., M. L. Kam, J. O. Washburn, and L. E. Volkman.** 1994. The insect tracheal system: a conduit for the systemic spread of *Autographa*

californica M nuclear polyhedrosis virus. Proc. Natl. Acad. Sci. USA **91:** 3224–3227.
10. **Fraser, M. J.** 1986. Ultrastructural observations of virion maturation in *Autographa californica* nuclear polyhedrosis virus infected *Spodoptera frugiperda* cell cultures. J. Ultrastruct. Mol. Struct. Res. **95:**189–195.
11. **Goh, D.** 1993. Identification and immunocharacterization of a 25K structural protein in *Autographa californica* nuclear polyhedrosis virus (AcMNPV). Virus Res. **28:**141–152.
12. **Harlow, E., and D. Lane.** 1988. Antibodies: a laboratory manual. Cold Spring Harbor Laboratory, Cold Spring Harbor, N.Y.
13. **Harrap, K.** 1972. The structure of nuclear polyhedrosis viruses. III. Virus assembly. Virology **50:**133–139.
14. **Hong, T., S. C. Braunagel, and M. D. Summers.** 1994. Transcription, translation, and cellular localization of PDV-E66: a structural protein of the PDV envelope of *Autographa californica* polyhedrosis virus. Virology **204:**210–222.
15. **Keddie, B. A., G. W. Aponte, and L. E. Volkman.** 1989. The pathway of infection of *Autographa californica* nuclear polyhedrosis virus in an insect host. Science **243:**1728–1730.
16. **Koerner, T. J., J. E. Hill, A. M. Myers, and A. Tzagoloff.** 1991. High-expression vectors with multiple cloning sites for construction of *trpE* fusion genes: pATH vectors. Methods Enzymol. **194:**477–490.
17. **Laemmli, U. K.** 1970. Cleavage of structural proteins during the assembly of the head of bacteriophage T4. Nature **227:**680–685.
18. **Lee, H. H., and L. K. Miller.** 1979. Isolation, complementation, and initial characterization of temperature-sensitive mutants of the baculovirus *Autographa californica* nuclear polyhedrosis virus. J. Virol. **31:**240–252.
19. **Li, Y., and L. K. Miller.** 1995. Expression and localization of a baculovirus protein phosphatase. J. Gen. Virol. **76:**2914–2948.
20. **Li, Y., and L. K. Miller.** 1995. Properties of a baculovirus mutant defective in the protein phosphatase gene. J. Virol. **69:**4533–4537.
21. **Lu, A., and E. B. Carstens.** 1991. Nucleotide sequence of a gene essential for viral DNA replication in the baculovirus *Autographa californica* nuclear polyhedrosis virus. Virology **181:**336–347.
22. **Lu, A., and L. K. Miller.** 1994. Identification of three late expression factor genes within the 33.8- to 43.4-map-unit region of *Autographa californica* nuclear polyhedrosis virus. J. Virol. **68:**6710–6718.
23. **Maeda, S., S. G. Kamita, and H. Kataoka.** 1991. The basic DNA-binding protein of *Bombyx mori* nuclear polyhedrosis virus—the existence of an additional arginine repeat. Virology **180:**807–810.
24. **Maniatis, T., E. F. Fritsch, and J. Sambrook.** 1982. Molecular cloning: a laboratory manual. Cold Spring Harbor Laboratory, Cold Spring Harbor, N.Y.
25. **McMaster, G., and G. Carmichael.** 1977. Analysis of single- and double-stranded nucleic acids on polyacrylamide and agarose gels by using glyoxal and acridine orange. Proc. Natl. Acad. Sci. USA **74:**4835.
26. **Monsma, S. A., A. G. P. Oomens, and G. W. Blissard.** 1996. The gp64 envelope fusion protein is an essential baculovirus protein required for cell-to-cell transmission of infection. J. Virol. **70:**4607–4616.
27. **Muller, R., M. N. Pearson, R. Russell, and G. F. Rohrmann.** 1990. A capsid-associated protein of the multicapsid nuclear polyhedrosis virus of *Orgyia pseudotsugata* genetic location, sequence, transcriptional mapping, and immunocytochemical characterization. Virology **176:**133–144.
28. **O'Reilly, D. R., L. K. Miller, and V. A. Luckow.** 1992. Baculovirus expression vectors: a laboratory manual. W. H. Freeman and Company, New York, N.Y.
29. **Passarelli, A. L., and L. K. Miller.** 1993. Three baculovirus genes involved in late and very late gene expression: ie-l, ie-n, and lef-2. J. Virol. **67:**2149–2158.
30. **Pearson, M. N., R. L. Q. Russell, G. F. Rohrmann, and G. S. Beaudreau.** 1988. P39, a major baculovirus structural protein: immunocytochemical characterization and genetic location. Virology **167:**407–413.
31. **Possee, R. D., T. P. Sun, S. C. Howard, M. D. Ayres, M. Hill-Perkins, and K. L. Gearing.** 1991. Nucleotide sequence of the *Autographa californica* nuclear polyhedrosis virus 9.4 kbp EcoRI-I and -R (polyhedrin gene) region. Virology **185:**229–241.
32. **Rohrmann, G. F.** 1992. Baculovirus structural proteins. J. Gen. Virol. **73:** 749–761.
33. **Russell, R. L. Q., and G. F. Rohrmann.** 1990. A baculovirus polyhedron envelope protein—immunogold localization in infected cells and mature polyhedra. Virology **174:**177–184.
34. **Sanger, F., S. Nicklen, and A. R. Coulson.** 1977. DNA sequencing with chain-terminating inhibitors. Proc. Natl. Acad. Sci. USA **74:**5463–5467.
35. **Stoltz, D., C. Pavan, and A. Da Cunha.** 1973. Nuclear polyhedrosis virus: a possible example of *de novo* intranuclear membrane morphogenesis. J. Gen. Virol. **19:**145–150.
36. **Theilmann, D., J. Chantler, S. Stewart, H. Flipsen, J. Vlak, and N. Crook.** 1996. Characterization of a highly conserved baculovirus structural protein that is specific for occlusion-derived virions. Virology **218:**148–158.
37. **Thiem, S. M., and L. K. Miller.** 1989. Identification, sequence, and transcriptional mapping of the major capsid protein gene of the baculovirus *Autographa californica* nuclear polyhedrosis virus. J. Virol. **63:**2008–2018.
38. **Vaughn, J. L., R. H. Goodwin, G. J. Tompkins, and P. McCawley.** 1977. The establishment of two cell lines from the insect *Spodoptera frugiperda* (Lepidoptera: Noctuidae). In Vitro **13:**213–217.
39. **Vialard, J. E., and C. D. Richardson.** 1993. The 1,629-nucleotide open reading frame located downstream of the *Autographa californica* nuclear polyhedrosis virus polyhedrin gene encodes a nucleocapsid-associated phosphoprotein. J. Virol. **67:**5859–5866.
40. **Volkman, L. E., P. A. Goldsmith, R. T. Hess, and P. Faulkner.** 1984. Neutralization of budded *Autographa californica* NPV by a monoclonal antibody: identification of the target antigen. Virology **133:**354–362.
41. **Wilson, M. E., T. H. Mainprize, P. D. Friesen, and L. K. Miller.** 1987. Location transcription and sequence of a baculovirus gene encoding a small arginine-rich polypeptide. J. Virol. **61:**661–666.
42. **Wolgamot, G. M., C. H. Gross, R. Russell, and G. F. Rohrmann.** 1993. Immunocytochemical characterization of p24, a baculovirus capsid-associated protein. J. Gen. Virol. **74:**103–107.
43. **Young, J. C., E. A. MacKinnon, and P. Faulkner.** 1993. The architecture of the virogenic stroma in isolated nuclei of Spodoptera frugiperda cells in vitro infected by *Autographa californica* nuclear polyhedrosis virus. J. Struct. Biol. **110:**141–153.